J. Eng. Technol. Sci., Vol. 53, No. 5, 2021, 210507

Thermal Performance Analysis of a Newly Designed Circular Firewood Boiling Salt Stove

Apichart Srichat[1], Weerapol Kaewka[1], Ponthep Vengsungnle[2], Songkran Wiriyasart[3] & Paisarn Naphon[3,*]

[1]Department of Mechanical Engineering, Faculty of Technology, Udon Thani Rajabhat University, Udon-Thani, 4100, Thailand
[2]Department of Agricultural Machinery Engineering, Faculty of Engineering and Architecture, Rajamangala University of Technology Isan, Nakhonratchasima 30000, Thailand
[3]Thermo-Fluids and Heat Transfer Enhancement Research Lab. (TFHT), Department of Mechanical Engineering, Faculty of Engineering, Srinakharinwirot University, Ongkharak, Nakhorn-Nayok, 26120, Thailand
*E-mail: paisarnn@g.swu.ac.th

Highlights:

- The thermal efficiency of the newly designed stove was higher than that of a traditional stove and an improved traditional stove.
- The final amounts of salt crystals and salt flowers obtained from the newly designed stove were higher compared to those obtained from the traditional stove and the improved stove.
- The payback periods were 50, 21, and 16 days for the traditional stove, the improved stove, and the newly designed stove, respectively.

Abstract. Different biomass stoves are introduced and distributed among people living in rural and urban areas, especially in developing countries. For salt crystal production in Thailand's rural north-eastern area, open fire stoves are used in domestic and small productive activities. Their thermal efficiency is very low for converting heat into utilization energy. A new stove with a circular configuration was designed and constructed to consider its thermal efficiency and economics, which were compared with those from a traditional and an improved traditional stove. The obtained thermal efficiency of the newly designed stove was 14.77% higher than that of the improved stove and 81.45% higher than that of the traditional stove. For the same initial saline volume, the final amounts of salt crystals and salt flowers obtained from the newly designed stove was higher compared with those obtained from the improved stove and the traditional stove, respectively, resulting in a 69.25% shorter payback period.

Keywords: *biomass; economic analysis; firewood; salt stove; thermal performance.*

Received August 26th, 2020, 1st Revision February 28th, 2021, 2nd Revision March 31st, 2021, Accepted for publication Juy 12th, 2021.
 ISSN: 2337-5779,
DOI: 10.5614/j.eng.technol.sci.2021.53.5.7

1 Introduction

Today, many people in the world still depend extensively on utilizing conventional solid fuels to meet their daily needs, especially for cooking. Firewood is often the only energy source for domestic and small productive activities. Traditionally, wood stoves are crude, low-efficiency combustion devices to obtain the required energy for cooking. Solid biomass fuel accounts for more than 80% of the total fuel used for domestic cooking and small productive activities. Because of the inefficiency of firewood stoves, the bulk of the energy released from burning firewood is lost, emitting large amounts of harmful pollutants. Inefficient burning of biomass fuel releases many pollutants such as particulate matter, PM2.5, black carbon, and carbon monoxide [1-3]. Improvement of the wood stove's low thermal efficiency has been done by considering wood stoves with different configurations [4] and by mapping the performance of firewood burning stoves [5-6]. A combined wood-burning stove/flue gas heat exchanger with an automatic closed-loop control system and numerical analysis have also been the subject of studies to improve the wood stove's thermal efficiency [7-9].

Different types of improved biomass stoves have been distributed to people in rural areas for domestic use in developing countries. Many researchers have attempted to increase the thermal performance of biomass stoves with different techniques. Higher-efficiency burning leads to reduced solid biomass fuel consumption. This improves people's health and livelihood and mitigates climate change by reducing the emission of different atmospheric pollutants and decreasing the burden on forests. Koyuncu & Pinar [10] and Maxwell, *et al.* [11] analyzed pollution and combustion of torrefied and raw biomass fuels in space-heating biomass stoves and investigated the thermal performance based on a traditional biomass stove in many places [12-14] with various improved techniques.

Roubik, *et al.* [15-16] developed a traditional biomass cooking stove in Vietnam. Bhattacharya, *et al.* [17] considered the effect of relevant parameters on cooking stove performance and pollutant emission. Kucerova, *et al.* [18] studied the thermal performance of wood-burning cooking stoves in Peru. Suresh, *et al.* [19] evaluated a biomass cooking stove's performance with different solid biomass fuel types using a heat pipe in the system [20]. Kshirsagar, *et al.* [21] applied a robust multi-response design for performance optimization of a hybrid draft biomass stove. However, as mentioned above, the thermal efficiency of these stoves is still lower than the thermal efficiency of stoves that use gas as fuel. Mitchell, *et al.* [22] improved the thermal performance of a cooking stove in Saharan Africa. Panwar & Rathore [23] designed a small 5-kW producer gas stove and a medium-scale gas stove with a two-layer porous radiant burner [24-

25] and LPG as fuel. Small-scale biogas plants and a methanol cooking stove have also been considered [26]. In rural areas, improved cooking stoves are generally made using easily available materials such as clay.

A chimney with a free draft technique was introduced to improve the thermal efficiency of a cooking stove to vent out pollutants generated due to incomplete combustion. Local biomass was used as fuel for these stoves [27-28]. Several studies have suggested that a combined heat and power stove system's improved thermal performance may be able to reduce biomass fuel consumption by using thermoelectrics [29-33]. Corn stoves with various biogases as fuel have also been studied [34-36].

All of the aforementioned literature attempted to overcome the two major drawbacks of traditional stoves, namely low efficiency and indoor air pollution. In Thailand, traditional firewood stoves with low thermal efficiency are also used in the salt boiling production process. This study aimed to enhance their thermal efficiency by adding baffles in order to increase the turbulent intensity and increase the duration of the hot gas flowing through the stove tunnel. Besides that, a new salt boiling firewood stove made of clay was designed and constructed to evaluate its thermal performance and economics. The obtained results were compared with those from a traditional stove and the improved stove.

2 Materials and Methods

2.1 Materials and Study Site

The Ban Dung area, Udon Thani province, is located in the north-eastern area of Thailand. The Ban Dung area lies between 17°24'54" N latitude and 102°47'12" E longitude. Experiments were performed with three different stove configurations: a traditional stove, an improved traditional stove, and a newly designed stove. In this area, the groundwater has a salty taste. Before the salt boiling production process, the saline used in the present study was sucked from the groundwater and collected until enough volume was obtained. Firewood as fuel for the salt boiling process was purchased from the rural wood market located in a nearby community.

2.2 Salt Stove Models Used in the Study

2.2.1 Traditional Stove

As shown in Figure 1, the traditional stove was a basic arrangement of clay earth blocks with dimensions of 240 x 600 x 80 cm, in which a tunnel runs horizontally. The stove was a U-shaped semi-enclosed mud stove with an opening in the front for feeding the firewood fuel and another end for exhaust gas outflow. The stove wall was coated with a thick layer of mud that was allowed to dry. The small humps at the top rim of the enclosure were used to provide support for the saline boiler and create an entry for secondary air, which is needed to combust the flammable gases.

2.2.2 Improved Stove

The improved stove was constructed the same as the traditional stove, with the same dimensions of 240 x 600 x 80 cm, resulting in a U-shaped semi-enclosed mud stove. The hot gas flows along the U-shaped stove tunnel like in the traditional stove and then rapidly flows out at the other end. The bulk of the energy from the burning firewood is lost with the exhaust gas. To reduce this loss, the hot gas's flow behavior inside the tunnel was improved by adding baffles in the improved stove. The baffles were fabricated from bricks, coated with clay with a height, width and length of 50 x 20 x 20 cm. The baffles were installed in the stove's inner wall in a staggered layout, as shown in Figure 1.

Figure 1 Configurations of the traditional and the improved stove.

2.2.3 Newly Designed Stove

The saline boiling bath capacity of the newly designed stove had to be the same as that of the traditional and the improved stove. Therefore, the newly designed stove was a circular configuration with inner and outer diameters of 410 cm and 430 cm, and a height of 80 cm, as shown in Figures 1-2. The wall stove was fabricated from bricks and mud and coated with a thick layer of mud. A fire is ignited in the open front with a width of 400 mm and the hot gas flow is distributed evenly inside the stove and then flows into the exhaust gas stack at the back of the stove. There is a rectangular column at the center of the stove to support the boiler, as shown in Figure 2.

Figure 2 Photograph of the saline boiling site of the circle stove.

2.3 Saline Used in the Work

Traditional stoves are usually constructed under open shades, thereby reducing emitted particle effects and gases on the community. Figure 1 shows that the saline boiler was fabricated from stainless steel with a dimension of 240 x 600 x 30 cm for the traditional and the improved stove. A boiler with an inner diameter of 430 cm and a height of 30 cm was used for the newly designed stove. The saline used in the present work was sucked from groundwater and collected until enough volume was obtained. For each batch with a volume of 4.32 m^3, saline with an initial salty level of 20% was boiled for 12.5 hours until the salt crystalized and salt flowers were formed. A hygrometer with an accuracy of 0.5% of full scale was used to measure the saline's salty level. During saline boiling, the saline inside the boiler was stirred with a paddle every 10 minutes to ensure a uniform overall temperature in the boiler, while the evaporation rate of the saline water was observed from the decreasing saline level inside the boiler.

2.4 Firewood Used in the Study

The firewood was collected and purchased from a local fuel wood market. All of the firewood was purchased at the same time in order to obtain consistent quality and moisture levels. A portable digital moisture meter with an accuracy of 0.5% of full scale was used to measure the firewood's moisture content. The firewood used in this study had an average moisture content of 27%. In order to maintain nearly the same airspace while burning in the salt stove, all firewood with an average low heating value of 15 MJ/kg was cut to the same size. The amount of firewood was measured using a digital scale with an accuracy of 0.1% of full scale. An anemometer with an accuracy of 0.1% of full scale was applied to measure the velocity of the inlet air. At the end of the test, the remaining firewood subtracted from the origin was used to determine the firewood feeding. The firewood feeding intervals were determined based on the flame's appearance; whenever the flame subsided, a new stock of firewood was added to the stove. Firewood feeding was continuously performed until the beginning of saline boiling, when the salt crystals and salt flowers started forming.

2.5 Experimental Method

2.5.1 Test Procedure

As shown in Figure 1, the salt boiling production process was performed with three different stove configurations, while trying to maintain the same initial relevant parameter values. For each batch with a volume of 4.32 m^3 and an initial salty level of 20%, saline was boiled for 12.5 hours. Before the start of the experiment, the initial relevant parameters were measured. The saline boiler was filled with the saline, and the firewood was ignited, after which the hot gas flowed into the stove tunnel. During the boiling process, the operators must scoop out saline impurities in order to obtain salt crystals and salt flowers without impurities. The salt flowers start forming first and float on the saline surface, while the salt crystals start forming later and sink to the boiler bottom. Therefore, the salt flowers were ladled with a boiler's paddle for drying in the open sun and the salt crystals were ladled later. The saline temperature, the stove temperature, and the exhaust gas temperature were measured by a k-type thermocouple with an accuracy of 0.1% of full scale. The saline's evaporated water was measured by observing the saline level during boiling with a stopwatch. The saline inside the boiler was stirred with a paddle every 10 minutes. The temperatures at various locations, as mentioned above, were recorded with a datalogger (DT800 Datataker) with an accuracy of 0.1% of full scale at regular intervals of an hour until the salt crystal and salt flowers started forming. The other parameters measured were firewood weight, firewood moisture content, evaporated water, and exhaust gas content.

2.5.2 Emission Measurement

Air pollutant measurements were also carried out to investigate CO, CO_2, and O_2 in the exhaust gas stack. When using a biomass stove, most of the salt stove procedures are performed by an operator who has experience with gradual feeding of the firewood and condition monitoring of the flame for the saline boiling process (especially in traditional stoves). This means that the operator is highly exposed to harmful gases emitted from the stove. Therefore, emission measurement was performed by locating a sensor in the stack at a height of 50-60 cm. The flue gas was measured by using a 1500-4500 portable combustion analyzer (4500 series).

Gas samples were taken through a gas probe using a diaphragm suction pump inside the instrument. The measuring probe has a sliding cone that allows the probe to be inserted in any stack with the gas probe tip roughly centered in the flue. The gas samples were cooled, dried, and cleaned of humidity and impurities/particulates by a condensate trap and a filter along with a rubber hose that connects the probe to the analyzer. Electrochemical gas sensors then analyzed the gas.

The electrochemical cell guarantees high precision results in a time interval of up to about 60 minutes, during which the instrument can be considered to be very stable. When the measurement takes a long time, during the zero calibrating phase, the instrument aspirates clean air from the environment and detects the sensors' drift from zero (20.9% for the O2 cell) and then compares them with the programmed values and compensates for them. The pressure sensor autozero must be done manually prior to measuring the pressure. The relevant values are measured and calculated by a microprocessor and viewed on an LCD, which is backlit to ensure easy reading even when lighting is poor.

3 Data Reduction

Heat added in the salt stove can be calculated from the combustion of firewood supplied to the salt stove as follows:

$$Q_{in} = m_f \cdot LHV \tag{1}$$

where Q_{in} is the combustion heat from the firewood (J), m_f is the weight of the firewood (kg), and LHV is the low heating value of the firewood (J/kg)

Heat utilization is the absorbed heat by the saline inside the boiler used in the process, which can be determined from the input heat minus the heat losses as follows:

$$Q_u = m_f \cdot LHV\text{-}Q_{loss} \tag{2}$$

Heat losses during the combustion process and through the stove tunnel consists of radiation loss, convection loss, wall loss, and exhaust gas loss as follows:

– convection loss

$$Q_{conv} = hA_{wall}(T_{wall}\text{-}T_{\infty}) \times \Delta t \tag{3}$$

– radiation loss

$$Q_r = \sigma\varepsilon A(T_W\text{-}T_{\infty})^4 \times \Delta t \tag{4}$$

– salt stove wall loss

$$Q_s = m_e C_{P,e} \Delta T \times \Delta t \tag{5}$$

– exhaust gas loss

$$Q_g = m_e C_{P,e} \Delta T \times \Delta t \tag{6}$$

where Q_{conv} is the convection loss (J), h is the heat transfer coefficient (W/m^2K), A_{wall} is the outside surface area of the stove (m^2), T_{wall} is the wall temperature (°C), T_{∞} is the surrounding temperature (°C), and Δt is the saline boiling time (s), Q_r is the radiation loss (J), ε is the Stefan-Boltzmann (5.67 x 10^{-8} W/m^2K), is the emissivity of the stove wall, Q_s is the stove wall loss (J), m_{wall} is the stove wall weight (kg), $C_{p,wall}$ is the specific heat of the stove wall (J/kg°C) , $T_{i,wall}$ is the inside wall temperature, $T_{o,wall}$ is the outside wall temperature, ΔT_{wall} is the temperature difference between the inside and the outside of the stove wall (°C), Q_g is the exhaust gas loss (J), $\dot{m}_e$ is the exhaust gas weight (kg), $C_{P,e}$ is the specific heat of the exhaust gas (J/kg °C), and T_e is the exhaust gas temperature (°C).

The thermal efficiency of the salt stove indicates the amount of fuel energy that is converted into utilization energy. The thermal efficiency of a salt stove can be defined as the ratio of the heat available for actual utilization to the theoretical heat produced by the complete combustion of the fuel. The thermal efficiency uncertainty is determined as follows:

$$\eta = \frac{Q_u}{Q_{in}} \times 100 = 1\text{-}\frac{Q_{loss}}{m_f \cdot LHV} \tag{7}$$

4 Accuracy and Uncertainty Analysis

The accuracy and uncertainty of the instruments are shown in Table 1. In the present study, the stove's thermal efficiency depended on the relevant parameters, as shown in Eq. (7). The uncertainty of thermal efficiency can be determined as follows:

$$\text{Uncertainty of } \eta = \sqrt{\begin{array}{l}\left(\frac{\partial\eta}{\partial \mathrm{T}_{o,wall}}\Delta t_{o,wall}\right)^2 + \left(\frac{\partial\eta}{\partial \mathrm{T}_{\infty}}\Delta T_{\infty}\right)^2 + \left(\frac{\partial\eta}{\partial \mathrm{T}_{o,wall}}\Delta t_{o,wall}\right)^2 + \left(\frac{\partial\eta}{\partial \mathrm{T}_{e}}\Delta T_{e}\right)^2 + \\ \left(\frac{\partial\eta}{\partial(\Delta t)}\Delta(\Delta T)\right)^2 + \left(\frac{\partial\eta}{\partial \mathrm{m}_{f}}\Delta m_{f}\right)^2 + \left(\frac{\partial\eta}{\partial \mathrm{m}_{wall}}\Delta m_{wall}\right)^2 + \left(\frac{\partial\eta}{\partial \mathrm{m}_{e}}\Delta m_{e}\right)^2 + \\ \left(\frac{\partial\eta}{\partial \mathrm{C}_{p,wall}}\Delta C_{p,wall}\right)^2 + \left(\frac{\partial\eta}{\partial \mathrm{C}_{p,wall}}\Delta C_{p,\mathrm{e}}\right)^2 + \left(\frac{\partial\eta}{\partial \mathrm{A}_{wall}}\Delta A_{wall}\right)^2\end{array}} \quad (8)$$

The properties of the relevant parameters, the uncertainty of the instruments, and the operating conditions are also required for calculation of the thermal efficiency uncertainty. By substituting Eq. (2) to Eq. (6) into Eq. (7), it can be found that the uncertainty of the thermal efficiency depends on eleven relevant parameters. The uncertainty of the thermal efficiency can be determined from Eq. (8). The calculation process is described as follows:

1. The first term in Eq. (8), $\left(\frac{\partial\eta}{\partial \mathrm{T}_{o,wall}}\right)$, Eq. (7) was differentiated from the outside wall temperature, while other terms were kept constant by using commercial software (Mathematica).
2. Calculation $\left(\frac{\partial\eta}{\partial \mathrm{T}_{o,wall}}\Delta t_{o,wall}\right)^2$ was performed by using the substituted relevant parameters.
3. The computation described above was then performed for the second term and the remaining terms until the last term.
4. The thermal efficiency uncertainty (Eq. (8)) was calculated.

The uncertainties of the measurement data and the relevant parameters were calculated with maximum uncertainties of ±5.5% of the thermal efficiency parameters (for more details, see the Coleman and Steel method [37]).

Table 1 Uncertainty and accuracy of instruments.

Instrument	Accuracy (%)	Uncertainly
Anemometer, m/s	0.1	±0.2
Moisture tester	0.5	±0.2
Hygrometer	0.5	±0.5
Thermocouple type-T	0.1	±0.1
Data logger (°C)	0.1	±0.2
Digital weighting scale, kg	0.1	±0.2

5 Results and Discussion

It was found that the total firewood fuel consumed by the three stoves was quite different, i.e. 1004 kg for the traditional stove, 799 kg for the improved stove, and 701 kg for the newly designed stove.

The hot gas flows through the stove tunnel in the traditional stove, transferring thermal energy to the salt boiler. Due to the baffles inside the improved stove, the hot gas flow period inside the stove tunnel is longer than in the traditional stove.

This means that the heat transfer from the hot gas to the saline inside the boiler also increases, consequently reducing the outlet exhaust gas temperature. The traditional stove's exhaust outlet gas temperature was approximately 420 °C, while for the improved stove it was 400 °C. The newly designed stove had the lowest exhaust gas temperature, 310 °C. This means that the utilization energy obtained from the newly designed stove for the salt boiling process was the highest compared to the two other stoves for the same input energy. In the present study, only three gases were present in the flue gas: CO, CO_2 and O_2 were measured and considered. It was found that the amount of CO from the traditional stove was the highest compared to that from the two other stoves. The maximum CO emissions from the traditional stove, the improved stove, and the newly designed stove were 3080, 2412 ppm, and 1,066 ppm, respectively. This may be because the area for incineration of firewood and hot gas distribution is greater in the newly designed stove than in the two other stoves. Therefore, the combustion process in the newly designed stove was better than in the improved stove and the traditional stove, leading to higher CO_2 and lower O_2 contents.

The amounts of salt crystals and salt flowers obtained from the newly designed stove were 4.11% and 5.99% higher than those from the improved stove and the traditional stove, respectively. In addition, the firewood used by the traditional stove was about 1004 kg for 10 hours, an average of 799 kg by the improved stove for 8 hours, and 701 kg by the newly designed stove for 8 hours, after which it was let to cool down. The variation of the stove temperature and saline temperature during the boiling process from the three stoves are shown in Figure 4. During the first 2-3 hours, the hot gas and saline temperatures sharply increased and then became relatively constant until the 10^{th} hour, when the temperatures tended to decrease. The maximum hot gas temperature inside the stove was approximately 531 °C for the traditional stove, 695 °C for the improved stove, and 727 °C for the newly designed stove, while the maximum temperatures of the saline inside the boiler were 106.85 °C, 107.40 °C, and 105.3 °C for the traditional stove, the improved stove, and the newly designed stove, respectively.

Figure 3 Photographs of the salt crystals and salt flowers.

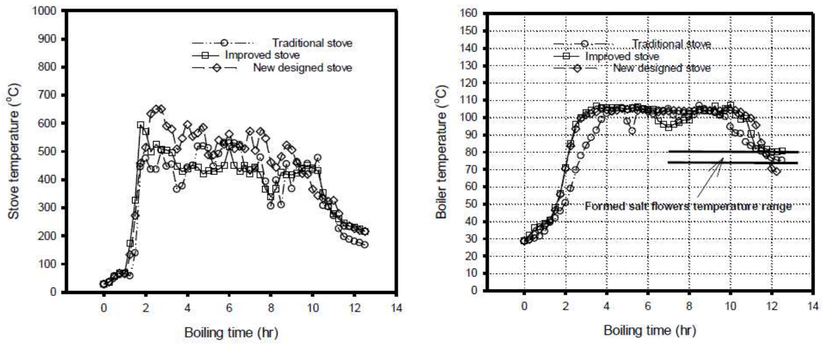

Figure 4 Variation of hot gas and saline temperatures with boiling time.

Figure 5 shows the energy balance obtained from the three stoves: convection loss, radiation loss, stove wall loss, exhaust gas loss, and front stove loss. For the improved stove, the exhaust gas loss was the highest (23.50%), followed by the stove wall loss (17.96%), the front stove heat loss (1.29%), the convection loss (0.14%), and the radiation loss (0.0001%), respectively. As compared with the traditional stove, the most reduced heat losses were the exhaust gas heat loss and the front stove heat loss, which resulted in 59.31% increased thermal efficiency. However, for the newly designed stove, the heat loss from the exhaust gas was the highest (20.10%), followed by the stove wall loss (12.63%), the front stove heat loss (1.19%), the convection loss (0.25%), and the radiation loss (0.0007%), respectively. It can be seen that the top-3 reduction heat losses for the newly designed stove were the exhaust gas heat loss, the stove wall heat loss, and the front stove heat loss, respectively.

Table 2 shows a comparison of the thermal efficiency obtained from the newly designed stove, the traditional stove, and the improved stove. It can be seen that the total consumed heat was 10,500 MJ, 11,969 MJ, and 15,039 KJ, respectively. In contrast, the utilization energy was 6,903 MJ, 6,855 MJ, and 5,499 MJ. This means that the newly designed stove had the highest thermal efficiency, with 65.74%, 57.28%, and 36.23% for the newly designed stove, the improved stove, and the traditional stove, respectively.

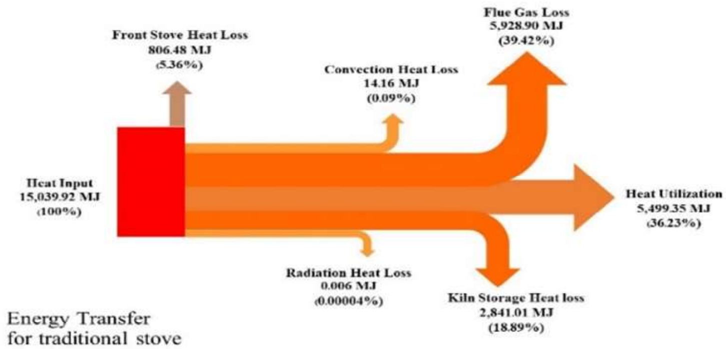

(A) Traditional stove

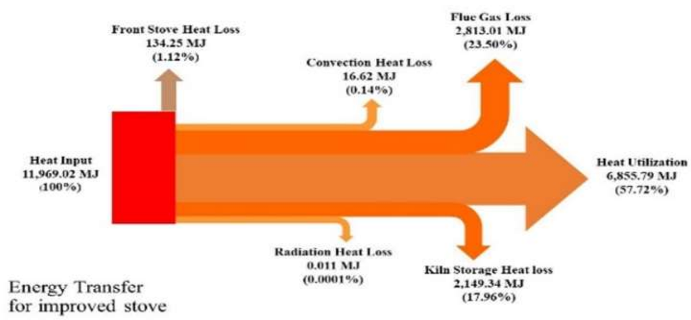

(B) Improved stove

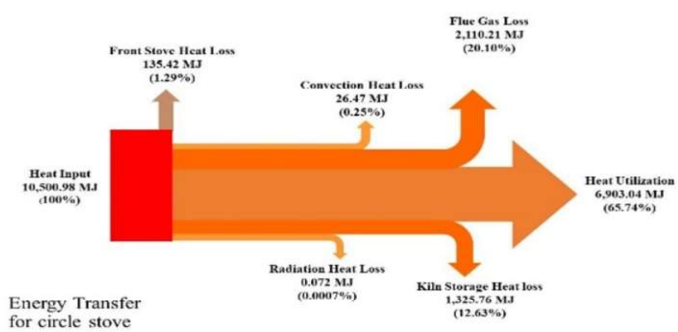

(C) A newly designed stove

Figure 5 Energy balance of three salt stoves (A) traditional stove, (B) improved stove, and (C) newly designed stove.

Table 2 Comparison of thermal efficiency obtained from three stoves.

Stoves	Supplied heat into the stove (MJ)	Utilization heat (MJ)	Thermal efficiency (%)
Traditional stove	15,039.92	5,449.35	36.23
Improved stove	11,969.02	6,855.79	57.28
Newly designed stove	10,500.98	6,903.04	65.74

For the economic analysis it was assumed that cost of the land and the building were not included. The salt boiling business investment costs included the cost of bricks, clay, labor, and equipment purchase. In contrast, the production cost or variable cost always depends on the production capacity per cycle, where the production cost includes the cost of saline and firewood. Income included salt crystal and salt flower sales.

The newly designed stove cost 66,000 Bath to construct, whereas the improved and the traditional stoves cost 61,500 and 62,000 Bath respectively. The production cost was 1,116, 1199, and 1373 Bath for the newly designed stove, the improved stove, and the traditional stove, respectively. The total income from the newly designed stove was the highest, at 5400 Bath, whereas for the improved stove and the traditional stove it was 4200 and 2600 bath, respectively.

$$\text{Payback period} = \frac{\text{Investment cost}}{\text{Profit per cycle}} = \frac{\text{Investment cost}}{\text{Income per cycle} - \text{Product cost}} \quad (9)$$

The payback period was calculated by assuming that the manufacturer runs 120 batches/year, however, it depends on the salt crystals and salt flower sales for each year. For the newly designed stove, the combined cost of saline and firewood for production was 133,920 Bath/year, whereas for the traditional stove the production cost was 164,760 Bath/year. Thus, the newly designed stove can help to save 30,840 Bath/year in fuel and saline costs.

The total income obtained from the newly designed stove was 648,000 Bath/year, while the total income of the traditional stove was 312,000 Bath/year. Thus, the newly designed stove can help to get 336,000 Bath/year more income. The payback period for the three different stoves can be calculated with Eq. (9).

From Table 3, the payback periods were 50, 21, and 16 days for the traditional stove, the improved stove, and the newly designed stove, respectively.

Table 3 Cost and payback period.

Details	Traditional stove	Improved stove	Newly designed stove	Unit
Investment	61,500	62,000	66,000	Bath
Total production cost per cycle	1,373.40	1,199.15	1,115.85	Bath
Total income per cycle	2,600.00	4,200.00	5,400.00	Bath
Profit per cycle (income per cycle minus production cost)	1,226.60	3,000.85	4,284.15	Bath
Payback period (investment/profit)	50.14	20.66	15.41	Day

6 Conclusion

Due to the inefficiency of traditional stoves for saline boiling, the bulk of the energy available is lost. Therefore, the improved thermal efficiency of a newly designed stove for saline boiling was presented in this paper. Also, an economic analysis of the newly designed stove was conducted. Reducing heat loss through the stove wall, openings, and flue gases are the new design's key points. Comparative parameters of the newly designed stove were used to compare its performance with that of a traditional stove and an improved traditional stove. Due to better combustion, the newly designed stove emits fewer pollutants than the improved stove and the traditional stove, resulting in lower firewood consumption. The newly designed stove had 14.77% and 81.45% higher thermal efficiency compared with the improved stove and the traditional stove, respectively. The obtained amounts of salt crystals and salt flowers were also increased, resulting in a shorter payback period. However, stoves cannot always reach the highest possible efficiency because they must be practical and thus must be continuously developed to obtain an optimum design for various applications.

Acknowledgments

The authors would like to express their appreciation to the Excellence Center for Sustainable Engineering (ECSE) of Srinakharinwirot University (SWU) for providing financial support for this study.

Nomenclature

A	outside surface area of the stove (m^2)	C_p	specific heat (J/kg°C)
h	heat transfer coefficient (W/m^2 °C)	H_{fg}	latent heat (J/kg)
LHV	low heating value (J/kg)	m	saline weight (kg)
Q_s	salt stove wall loss (J)	Q_{conv}	convection loss (J)
Q_g	exhaust gas loss (J)	Q_{in}	heat from firewood (J)
Q_r	radiation loss (J)	Q_u	utilization heat (J)
T	temperature (°C)	Δt	saline boiling time (s)
$\boldsymbol{\sigma}$	Stefan-Boltzmann (5.67 x 10^{-8} W/m^2 °C)	$\boldsymbol{\varepsilon}$	emissivity of the stove (-)
ΔT	temperature difference (°C)		

Subscripts

conv	convection	*e*	exhaust gas
f	firewood	*in*	inside
wall	wall	*max*	maximum
out	outside	*s*	evaporated water
∞	surrounding		

References

[1] Rupakheti, D., Oanha, N.T.K., Rupakheti, M., Sharma, R.K., Panday, A.K., Puppala, S.P. & Lawrence, M.G., *Indoor Levels of Black Carbon and Particulate Matters in Relation to Cooking Activities Using Different Cook Stove-Fuels in Rural Nepal,* Energy for Sustainable Development, **48**, pp. 25-33, 2019.

[2] Roubík, H. & Mazancov, J., *Small-scale Biogas Plants in Central Vietnam and Biogas Appliances with a Focus on a Flue Gas Analysis of Biogas Cook Stoves,* Renewable Energy, **131**, pp. 1138-1145, 2019.

[3] Deng, M., Li, P., Ma, R., Shan, M. & Yang, X., *Air Pollutant Emission Factors of Solid Fuel Stoves and Estimated Emission Amounts in Rural Beijing,* Environment International, **138**, 105608, 2020.

[4] Skreiberg, O. & Georges, L., *Wood Stove Material Configurations for Increased Thermal Comfort,* Energy Procedia, **142**, pp. 488-494, 2014.

[5] Carvalhoa, R.L., Jensena, O.M. & Tarelho, L.A.C., *Mapping the Performance of Wood-Burning Stoves by Installations Worldwide*, Energy and Buildings, **127**, pp. 658-679, 2016.

[6] Carvalho, R.L., Vicente, E.D., Tarelho, L.A.C. & Jensen, O.M., *Wood Stove Combustion Air Retrofits: A Low Cost Way to Increase Energy Savings in Dwellings,* Energy & Buildings, **164**, pp. 140-152, 2018.

[7] Cable, A., Georges, L., Peigne, P., Skreiberg, O. & Druette, L., *Evaluation of A New System Combining Wood-Burning Stove, Flue Gas Heat Exchanger and Mechanical Ventilation with Heat Recovery in Highly Insulated Houses,* Applied Thermal Engineering, **157**, 113693, 2019.

[8] Illerup, J.B., Hansen, B.B., Lin, W., Nickelsen, J., Pedersen, V.H., Eskerod, B. & Johansen, K.D., *Performance of an Automatically Controlled Wood Stove: Thermal Efficiency and Carbon Monoxide Emissions*, Renewable Energy, **151**, pp. 640-647, 2020.

[9] Scharler, R., Gruber, T., Ehrenhöfer, A., Kelz, J., Bardar, R.M., Bauer, T., Hochenauer, C. & Couce, A.A., *Transient CFD Simulation of Wood Log Combustion in Stoves,* Renewable Energy, **145**, pp. 651-662, 2020.

[10] Koyuncu, T., & Pinar, Y., *The Emissions from a Space-Heating Biomass Stove,* Biomass and Bioenergy, **31**, pp. 73-79, 2007.

[11] Maxwell, D., Gudka, B.A., Jones, J.M. & Williams, A., *Emissions From the Combustion of Torrefied and Raw Biomass Fuels in a Domestic Heating Stove*, Fuel Processing Technology, **199**, 106266, 2020.

[12] Wang, Z., Duanmu, L., Yuan, P., Ning, M. & Liu, Y., *Experimental Study of Thermal Performance Comparison Based on the Traditional and Multifunctional Biomass Stoves in China,* Procedia Engineering, **121**, pp. 845 - 853, 2015.

[13] Phusrimuang, J. & Wongwuttanasatian, T., *Improvements On Thermal Efficiency of a Biomass Stove for a Steaming Process in Thailand*, Applied Thermal Engineering, **98**, pp. 196-202, 2016.

[14] Rasoulkhani, M., Ebrahimi-Nik, M., Abbaspour-Fard, M.H. & Rohani, A., *Comparative Evaluation of the Performance of an Improved Biomass Cook Stove and the Traditional Stoves of Iran,* Sustainable Environment Research, **28**, pp. 438-443, 2018.

[15] Roubik, H., Mazancova. J., Pung L.D. & Dung D.V., *Quantification of Biogas Potential from Livestock Waste in Vietnam*, Argonomy Research, **15**, pp. 540-552, 2017.

[16] Roubik, H., Barrera, S., Dung D.V., Phung, L.D. & Mazancova J., *Emission Reduction Potential of Household Biogas Plants in Developing Countries: The Case of Central Vietnam*, Journal of Cleaner Production, **270**, 122257, 2020.

[17] Bhattacharya, S.C., Albina, O.D. & Khaing, A.M., *Effects of Selected Parameters on Performance and Emission of Biomass-fired Cookstoves*, Biomass and Bioenergy, **23** pp. 387-395. 2002.

[18] Kucerova I., Banout, J., Lojka, B. & Polesny, Z., *Performance Evaluation of Wood Burning Cookstoves in Rural Area Near Pucallpa, PERU*, Environmental Engineering and Management Journal, **15**, pp. 2421-2428, 2016.

[19] Suresh, R., Singh, V.K., Malik, J.K., Datta, A. & Pal, R.C., *Evaluation of The Performance of Improved Biomass Cooking Stoves with Different Solid Biomass Fuel Types*, Biomass and Bioenergy, **95**, pp. 27-34, 2016.

[20] Tanaka, H., *Thermal Distillation System Utilizing Biomass Energy Burned in Stove by Means of Heat Pipe*, Alexandria Engineering Journal, **55**, pp. 2203-2208, 2016.

[21] Kshirsagar, M.P. & Kalamkar, V.R. *Application of Multi-response Robust Parameter Design for Performance Optimization of a Hybrid Draft Biomass Cook Stove*, Renewable Energy, **153**, pp. 1127-1139, 2020.

[22] Mitchell, E.J.S., Ting, Y., Allan, J., Lea-Langton, A.R., Spracklen, D.V., McFiggans, G., Coe, H., Routledge, M.N., Williams, A. & Jones, J.M., *Pollutant Emissions from Improved Cookstoves of the Type Used in Sub-Saharan Africa*, Combustion Science and Technology, **192**, pp. 1582-1602, 2020.

[23] Panwar, N.L. & Rathore, N.S., *Design and Performance Evaluation of a 5kW Producer Gas Stove*, Biomass and Bioenergy, **32**, pp. 1349-1352, 2008.
[24] Kaushik, L.K. & Muthukumar, P., *Life Cycle Assessment (LCA) and Technoeconomic Assessment (TEA) of Medium Scale (5-10 kW) LPG Cooking Stove with Two-layer Porous Radiant Burner*, Applied Thermal Engineering, **133**, pp. 316-326, 2018.
[25] Mishra, N.K., Subhash, A., Mishra, C. & Muthukumar, P., *Performance Characterization of a Medium-Scale Liquefied Petroleum Gas Cooking Stove with a Two-layer Porous Radiant Burner*, Applied Thermal Engineering, **89**, pp. 44-50, 2015.
[26] Makonese, T., Annegarn, H.J. & Meyer, J., *Performance Evaluation of Three Methanol Stoves Using a Contextual Testing Approach*, Energy for Sustainable Development, **55**, pp. 13-23, 2020.
[27] Tryner, J., Willson, B.D. & Marchese, A.J., *The Effects of Fuel Type and Stove Design on Emissions and Efficiency of Natural-Draft Semi-Gasifier Biomass Cook Stoves*, Energy for Sustainable Development, **23**, pp. 99-109, 2014.
[28] Raman, P., Murali, J., Sakthivadivel, D. & Vigneswaran, V., *Performance Evaluation of Three Types of Forced Draft Cook Stoves Using Fuel Wood and Coconut Shell*, Biomass and Bioenergy, **49**, pp. 333-340, 2013.
[29] Montecuccoa, A., Sivitera, J. & Knoxa, A.R., *A Combined Heat and Power System for Solid-Fuel Stoves Using Thermoelectric Generators*, Energy Procedia, **75**, pp. 597-602, 2015.
[30] Najjar, Y.S.H. & Kseibi, M.M., *Heat Transfer and Performance Analysis of Thermoelectric Stoves*, Applied Thermal Engineering, **102**, pp. 1045-1058, 2016.
[31] Gao, H.B., Huang, G.H., Li, H.J., Qu, Z.G. & Zhang, Y.J., *Development of Stove Powered Thermoelectric Generators: A Review,* Applied Thermal Engineering, **96**, pp. 297-310, 2016.
[32] Montecucco, A., Siviter, J. & Knox, A.R., *Combined Heat and Power System for Stoves with Thermoelectric Generators*, Applied Energy, **185**, pp. 1336-1342, 2017.
[33] Guoneng, L., Youqu, Z., Hongkun, L., Jiangen, H., Jian, L., & Wenwen, G., *Micro Combined Heat and Power System Based on Stove-Powered Thermoelectric Generator*, Renewable Energy, **155**, pp. 160-171, 2020.
[34] Yuan, H., Song, X., Guan, R., Zhang, L., Li, X. & Zuo, X., *Effect of Low Severity Hydrothermal Pretreatment on Anaerobic Digestion Performance of Corn Stover*, Bioresource Technology, **294**, 122238, 2019.
[35] Shaoa, L., Chena, H., Lia, Y., Lic, J., Chena, G. & Wanga, G., *Pretreatment of Corn Stover via Sodium Hydroxide-Urea Solutions to Improve the Glucose Yield*, Bioresource Technology, **307**, 123191, 2020.

[36] Valsero, M.H., Cambronero, J.G., García, A.I.P. & Antolínez, R.D., *A Global Approach to Obtain Biobutanol from Corn Stover,* Renewable Energy, **148**, pp. 223-233, 2020.
[37] Coleman, H.W. & Steele, W.G., *Experimental and Uncertainty Analysis for Engineers*, John Wiley & Sons, New York, 1989.